Enhancement of Intermittency in Superfluid Turbulence

Laurent Boué, Victor L'vov, Anna Pomyalov, and Itamar Procaccia
Department of Chemical Physics, Weizmann Institute of Science, Rehovot 76100, Israel
(Received 26 July 2012; published 4 January 2013)

We consider the intermittent behavior of superfluid turbulence in ^{4}He. Because of the similarity in the nonlinear structure of the two-fluid model of superfluidity and the Euler and Navier-Stokes equations, one expects the scaling exponents of the structure functions to be the same as in classical turbulence for temperatures close to the superfluid transition T_λ and also for $T \ll T_\lambda$. This is not the case when the densities of normal and superfluid components are comparable to each other and mutual friction becomes important. Using shell model simulations, we propose that in this situation there exists a range of scales in which the effective exponents indicate stronger intermittency. We offer a bridge relation between these effective and the classical scaling exponents. Since this effect occurs at accessible temperatures and Reynolds numbers, we propose that experiments should be conducted to further assess the validity and implications of this prediction.

DOI: 10.1103/PhysRevLett.110.014502 PACS numbers: 47.37.+q, 67.25.dm

Introduction.—Nonequilibrium systems are often characterized by relatively quiescent periods which are interrupted by rare but violent changes of the physical observables. This generic phenomenon is referred to as "intermittency." Accepting Richardson's idea of a step-by-step energy cascade in highly excited hydrodynamic turbulence, Kolmogorov conjectured [1] that after many steps of the cascade the small scale turbulence becomes locally isotropic and space homogeneous, obeying universal statistics, independently of the turbulence excitation mechanisms. Since then the investigation of the universal properties of fully developed hydrodynamic turbulence became an active field with many remaining open questions. In the inertial interval of scales $L \gg r \gg \eta$, the intermittent behavior of turbulence can be studied in terms of scale-invariant velocity structure functions:

$$S_p(r) \equiv \langle |\boldsymbol{v}(\boldsymbol{R}, t) - \boldsymbol{v}(\boldsymbol{R} + \boldsymbol{r}, t)|^p \rangle \propto r^{\xi_p}, \qquad (1)$$

and its p-order exponents ξ_p. Here $\langle \cdots \rangle$ denotes a time averaging, L is the energy input scale, e.g., due to flow instabilities, and η is the viscous energy dissipation scale.

In 1941 Kolmogorov assumed that in the inertial interval the energy flux over the scales ε is the only relevant parameter [1]. Then the scaling of $S_p(r)$ follows from dimensional reasoning: $S_p^{\mathrm{K41}}(r) \simeq (\varepsilon r)^{p/3}$. While K41 low-order exponents $\xi_p^{\mathrm{K41}} = p/3$ are close to observations (compare $\xi_2^{\mathrm{K41}} = 2/3 \approx 0.67$ with the experimental $\xi_2^{\mathrm{exp}} \simeq 0.70$), for $p > 3$, $\xi_p^{\mathrm{exp}} < \xi_p^{\mathrm{K41}}$, and the discrepancy increases with p, indicating that in reality the statistics of turbulence is not scale invariant. In particular, in the K41 framework $S_p(r)/[S_2(r)]^{p/2}$ is r independent, like in Gaussian statistics, while the observed ratios $S_p(r)/[S_2(r)]^{p/2}$ increase with r. This means that the probability of observing large values of small scale velocity fluctuations [that mainly contribute to $S_p(r)$ with large p] significantly exceeds its normal K41 level; i.e., the small scale turbulent flow is strongly intermittent. Turbulence in superfluid ^{3}He and ^{4}He merges traditional fluid mechanics with low-temperature physics. Unlike classical fluids, where the circulation around the vortices is a dynamical variable, in superfluids it is quantized to integer values of $\kappa = h/m$. Here h is Planck's constant and m is the mass of a superfluid particle. This leads to the appearance of an additional length scale ℓ, the mean intervortex distance. At scales $r \gg \ell$ superfluids can be described as two interpenetrating entities with two different velocities: $\boldsymbol{v}_s$ (inviscid superfluid component) and $\boldsymbol{v}_n$ (normal component), and temperature dependent densities $\rho_s(T)$ and $\rho_n(T)$ interacting via the so-called mutual friction force [2–8].

An important question concerns the analogies between superfluid and classical turbulence. The pioneering experiments of Maurer and Tabeling suggest that intermittency is also present in turbulent superfluid ^{4}He [9]. This crucial observation implies that the intermittency is not caused by the particular structure of the Navier-Stokes equations and thus superfluid turbulence offers an additional case to investigate its physical mechanisms. Unfortunately, intermittency in superfluids has received far less attention than in classical turbulence [10]. The aim of this Letter is to compare intermittency in ^{4}He-superfluid turbulence with classical turbulence. An important parameter characterizing superfluid turbulence is the ratio ρ_s/ρ_n. For T slightly below the phase transition temperature T_λ, when $\rho_s/\rho_n \ll 1$, one can neglect the superfluid component and the statistics of turbulent superfluid ^{4}He becomes close to that of classical fluids. We also expect similar inertial range behavior of classical and superfluid turbulence for $T \ll T_\lambda$, when $\rho_n \ll \rho_s$, due to the inconsequential role played by the normal component; see, e.g., Ref. [10]. Moreover (and less trivially), the intermittent scaling exponents ξ_p have to be the same in classical and low-temperature superfluid turbulence. This is because the

nonlinear structure of the equation for the superfluid component is the same as the Euler equation, and dissipative mechanisms are believed to be irrelevant. Accordingly, we focus in on the range of $T \simeq (0.8\text{–}0.9)T_\lambda$, where $\rho_s \sim \rho_n$, and compare it to the high and low T limits, when $\rho_s/\rho = 0.1$ and 0.9, respectively. Here $\rho = \rho_s + \rho_n$ is the total density of the superfluid. Our main tool is numerical simulations of superfluid turbulence in the two-fluid model [2] simplified further using a shell model [11–13]. Shell models give in the classical case, with the right choice of parameters, scaling exponents which are close to the experimental values $\xi_2^{\rm num} = 0.72$ versus $\xi_2^{\rm exp} = 0.70$, $\xi_4^{\rm num} = 1.26$ versus $\xi_4^{\rm exp} = 1.28$, etc.

The main result of the Letter is as follows. For temperatures such that $\rho_s/\rho \lesssim 0.1$ and $\rho_s/\rho \gtrsim 0.9$, the scaling behavior of superfluid turbulence is practically the same as in classical fluids. However, for temperatures such that $\rho_s/\rho \simeq 0.5\text{–}0.75$, we discover the emergence of a wide (up to 3 decades) interval of scales characterized by different effective scaling exponents $\tilde{\xi}_p \neq \xi_p^{\rm num}$. For example, when $\rho_s = \rho_n$, the value of $\tilde{\xi}_2$ diminishes from its intermittent value $\xi_2^{\rm num} \approx 0.72$ down to $\tilde{\xi}_2 \approx 0.67$, close to the K41 value $\xi_2^{\rm K41} = 2/3$. At the same time, the exponents $\tilde{\xi}_p$ for $p > 3$ deviate further from the K41 values: $\tilde{\xi}_p < \xi_p^{\rm num} < \xi_p^{\rm K41}$. This fact can be considered as enhancement of intermittency in superfluid turbulence compared to the classical case.

In addition, based on numerical observations that the probability distribution function (PDF) of the normalized shell energy is temperature independent, we suggest the relation between effective and classical exponents:

$$\tilde{\xi}_p = \xi_p^{\rm num} - p(\xi_2^{\rm num} - \tilde{\xi}_2)/2 \approx \xi_p^{\rm num} - 0.026p, \quad (2)$$

which is in good agreement with observed values of $\tilde{\xi}_p$.

Numerical procedure.—Shell models of superfluid turbulence [14,15] are simplified caricatures of the Navier-Stokes and Euler equations in $\boldsymbol{k}$ representation:

$$\left[\frac{d}{dt} + \nu_n k_m^2\right] u_m^n = \mathrm{NL}[u_m^n] + F_m^n + f_m^n, \quad (3a)$$

$$\left[\frac{d}{dt} + \nu_s k_m^2\right] u_m^s = \mathrm{NL}[u_m^s] - F_m^s + f_m^s, \quad (3b)$$

$$\mathrm{NL}[u_m] = i(a k_{m+1} u_{m+2} u_{m+1}^* + b k_m u_{m+1} u_{m-1}^* - c k_{m-1} u_{m-1} u_{m-2}), \quad (3c)$$

They mimic the statistical behavior of $\boldsymbol{k}$ Fourier components of the turbulent superfluid and normal velocity fields in the entire shell of wave vectors $k_m < k < k_{m+1}$ by the complex shell velocities $u_m^{n,s}$. The shell wave numbers are chosen as a geometric progression $k_m = k_0 \lambda^m$, where $m = 1, 2, \ldots, M$ are the shell indexes and $\lambda = 2$ is the shell-spacing parameter. The value of the reference shell wave number k_0 affects the typical time scales, but otherwise is arbitrary. We used $k_0 = 1/16$. Similarly to the Navier-Stokes equation, the $\mathrm{NL}[u_m]$ term in Eq. (3c) is quadratic in velocities, proportional to k, and conserves the kinetic energy $E = \frac{1}{2}\sum_m |u_m|^2$ (in the forceless, inviscid limit) provided that $a + b + c = 0$. We used the Sabra version [12] of $\mathrm{NL}[u_m]$ with $b = c = -a/2$, $a = 1$, which ensures [11,12] that $\xi_p^{\rm num}$ are close to $\xi_p^{\rm exp}$.

The coupling terms $F_m^{n,s} = \alpha_{n,s}\Omega_s(u_m^s - u_m^n)$ with $\Omega_s^2 \equiv \sum_m k_m^2 |u_m^s|^2$, and $\alpha_s = \alpha$, $\alpha_n = \alpha\rho_s/\rho_n$ [14,15], account for the mutual friction between normal and superfluid velocities and are proportional to the known temperature dependent mutual friction parameter $\alpha(T)$.

In Eq. (3a), ν_n is the kinematic viscosity of the normal component. It is known that vortex reconnections act as an energy sink in superfluids. The details of this complicated and otherwise still not fully understood dissipation process go beyond the scope of this Letter. We modeled it by adding in Eq. (3b) an effective superfluid viscosity $\nu_s \ll \nu_n$. Unlike our previous work [15], we did not use the hyperviscosity to avoid the possible numerical artifacts associated with the too strong onset of the damping of the velocity at the dissipative scales. The simulations were carried out for $M = 28\text{–}46$ and $\nu_s/\nu_n \simeq 10^{-6}\text{–}10^{-2}$ at different temperatures. As long as $\nu_s/\nu_n \ll 1$, the actual value of ν_s only slightly affects the form of the superfluid spectrum at scales smaller than ℓ, where the hydrodynamic description is no longer valid. The results below were obtained with $M = 36$ shells, $\nu_s = 10^{-12}$ and $\nu_n = 10^{-10}$. These parameters allowed us to clearly resolve subregions with different scaling behavior.

To sustain the steady state we used a δ correlated in time random forcing $f_m^{s,n}$ in the first two shells with amplitudes $f_1 = 0.01$, $f_2 = \sqrt{-(c/a)}f1$ [15] for both normal and superfluid components. Equations (3a)–(3c) were solved using the 4th order Runge-Kutta method [16]. The time evolution was followed for about a hundred forcing scale eddy-turnover times. The Taylor-scale Reynolds number at all temperatures was about $\mathrm{Re}_\lambda = 5 \times 10^5$. The parameters used in simulations are shown in Table I.

Results and discussions.—Firstly, we study the scaling of the velocity structure functions (1) defined in the shell models as $S_p^{s,n}(k_m) \equiv \langle |u_m^{s,n}|^p \rangle$. We also defined for convenience the structure functions $C_p(k_m) \equiv k_m^{\xi_p^{\rm num}} S_p(k_m)$ compensated by the classical anomalous scaling.

Figure 1(a) shows $C_2(k_m)$. The almost horizontal lines for $\rho_s/\rho = 0.9$ and 0.1 indicate the usual intermittent scaling behavior. However, for $\rho_s/\rho = 0.5$ one detects

TABLE I. The model parameters. The values of T/T_λ and α were interpolated using the experimental data in Ref. [17].

ρ_s/ρ	0.1	0.25	0.4	0.5	0.6	0.65	0.7	0.75	0.9
T/T_λ	0.99	0.97	0.93	0.90	0.87	0.84	0.82	0.79	0.677
α	1.09	0.51	0.314	0.25	0.22	0.175	0.155	0.14	0.07
$\alpha\rho/\rho_n$	1.21	0.68	0.52	0.50	0.49	0.50	0.52	0.54	0.67

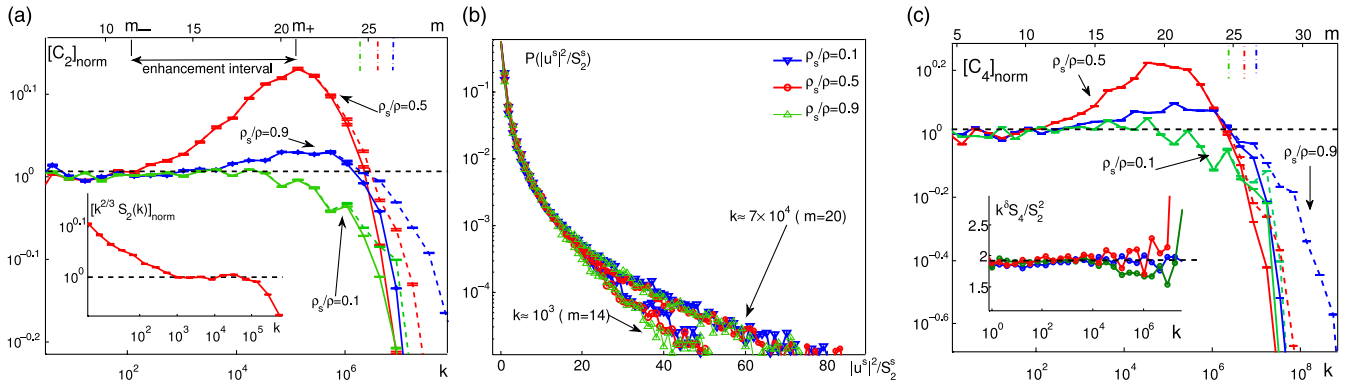

FIG. 1 (color online). (a) The compensated structure functions $C_2^{n,s}(k_m)$ for $\rho_s/\rho = 0.1$, 0.5, and 0.9, normalized by their mean values over shells with $m = 7$–12. Inset: $k^{2/3}S_2(k_m)$ normalized by its mean value over $m = 15$–20 for $\rho_s/\rho = 0.5$. Solid lines show the normal component, dashed lines show the superfluid components. The upper axis is marked with the shell numbers, the lower axis shows the corresponding wave numbers. (b) Demonstration of the temperature independence of the PDFs for shells $m = 14$ and $m = 20$. (c) The normalized compensated $C_4^{n,s}(k_m)$. Inset: The collapse of $k^\delta S_4(k)/[S_2(k)]^2$, compensated using classical exponents $\delta \equiv 2\xi_2^{\rm num} - \xi_4^{\rm num} \approx 0.184$. The horizontal black dashed lines serve to guide the eye only. Color code is the same in all panels. Vertical dot-dashed lines in (a) and (c) denote the intervortex scale $1/\ell$ (see Ref. [14]).

the emergence of a wide enhancement interval where the energy accumulates and where $\tilde{\xi}_2 \simeq 2/3$ [18] . This is clearly seen in the inset, where $S_2(k_m)$ is compensated with K41 scaling. At first glance, the scaling with $\tilde{\xi}_2 \simeq \xi_2^{\rm K41} = 2/3$ can be considered as the normal K41 scaling in superfluids. In this case one would expect that the PDF of normalized energy in m shell $P^{n,s}[|u_m^{n,s}|^2/S_2^{n,s}(k_m)]$ should collapse for all m. This is, however, *not* the case here. Figure 1(b) shows that the PDFs for different m are in fact very different from each other. The much longer tails associated with larger values of k_m reveal strong intermittency effects confirmed in Fig. 1(c), where $C_4^{n,s}(k_m)$ is almost flat for $\rho_s/\rho = 0.9$ and 0.1, but show a different scaling for $\rho_s/\rho = 0.5$ with $\tilde{\xi}_4 \approx 1.21 < \xi_4^{\rm num} = 1.256 < \xi^{\rm K41} = 4/3$. The next order structure functions, $S_6(k)$, $S_8(k)$, ..., demonstrate the same type of behavior with $\tilde{\xi}_p$ deviating even further away from the K41 values than $\xi_p^{\rm num}$ in classical fluids.

Another important observation in Fig. 1(b) is that the PDFs are practically temperature independent. Then knowing $\xi_p^{\rm num}$ and $\tilde{\xi}_2$, we can predict with very good accuracy all other $\tilde{\xi}_p$. Comparing the expressions for $S_p^{n,s}(k_m)$,

$$S_p^{n,s}(k_m) = \int_0^\infty \mathcal{P}^{n,s}[|u_m^{n,s}|^2/S_2^{n,s}(k_m)]|u_m^{n,s}|^p du_m^{n,s},$$

in the regions of different scaling, one arrives after some simple algebra to Eq. (2). An immediate consequence of Eq. (2) is that the ratio $S_p(k)/[S_2(k)]^{p/2}$ is the same in the regions with $\xi_p^{\rm num}$ and $\tilde{\xi}_p$ scaling. This prediction fully agrees with observations [see, e.g., inset in Fig. 1(c) for $p = 4$] and thus lends strong support to Eq. (2).

To quantify the intermittency enhancement we define $\Psi_2 \equiv \log_2\{[\max_m C_2(k_m)/\langle C_2(k_m)\rangle]\}$, where $\langle C_2(k_m)\rangle$ is the mean value of $C_2(k_m)$ on the plateau. In Fig. 2 we display the T and ρ_s/ρ dependence of Ψ_2 and $\tilde{\xi}_2$. Denote by $m_\pm$ the left and right edges of the enhancement interval and its extent as $k_{m_+}/k_{m_-} = 2^{\Delta m}$, $\Delta m \equiv (m_+ - m_-)$. Then, using data in Fig. 2 and computing the ratios $\Psi(T)/[\xi_2^{\rm num} - \tilde{\xi}_2(T)] \equiv \Delta m$ for all T, we found that $\Delta m \simeq 8$–10 is practically independent of T. In other words, the extent of the enhancement interval $k_{m_+}/k_{m_-} = 2^{\Delta m} \simeq 250$–1000.

As expected, significant intermittency enhancement takes place for $\rho_s \sim \rho_n$ [or more precisely $\rho_s \simeq (0.4$–$0.8)\rho$—see Fig. 2] when the two-fluid model (3) differs mostly from a single classical fluid. Normal and superfluid components in Eqs. (3a)–(3c) are coupled by the mutual friction force $F_m \propto \alpha(u_m^s - u_m^n)$ which causes the energy exchange between normal and superfluid components and the energy dissipation. Thus these two phenomena are the only possible reasons for the observed intermittency enhancement and

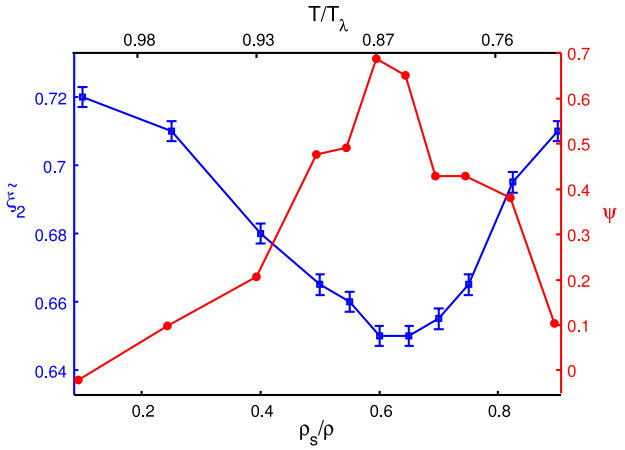

FIG. 2 (color online). T/T_λ and $\rho_s(T)/\rho$ dependencies (upper and lower axes) of the exponent $\tilde{\xi}_2$, left axis, and the enhancement magnitude Ψ, right axis. The maximum of $\Psi_2 \approx 0.7$ and minimum of $\tilde{\xi}_2 \approx 0.65$ are reached at $T \approx 0.865T_\lambda$ ($\rho_s \approx 0.6\rho$).

both disappear in the case of full velocity locking $u_m^s(t) = u_m^n(t)$. Velocity locking can be statistically quantified by the cross-correlation coefficient of normal and superfluid velocities:

$$\mathcal{K}_m \equiv \langle [u_m^{s*} u_m^n + u_m^s u_m^{n*}] \rangle / \langle [u_m^{s*} u_m^s + u_m^n u_m^{n*}] \rangle.$$

For $\mathcal{K}(k_m) = 0$, the superfluid and normal components are statistically independent subsystems, while for $\mathcal{K}(k_m) = 1$ they are completely locked to each other. Clearly, only for $0 < \mathcal{K}(k_m) < 1$ can we expect intermittency enhancement. A result of Ref. [20] for the correlation coefficients can be reformulated for shell model

$$\mathcal{K}_m \simeq \frac{2[\alpha_n S_{2,m}^s + \alpha_s S_{2,m}^n]/[S_{2,m}^s + S_{2,m}^n]}{\alpha_n + \alpha_s + k_m[\nu_n k_m + S_{2,m}^s + S_{2,m}^n]/\sqrt{\langle \Omega_s^2 \rangle}}.$$

Here, $S_{2,m}^n \equiv S_2^n(k_m)$ and similarly for $S_{2,m}^s$. Analysis of this equation shows that the v_m^s and v_m^n are locked when $k_m \eta \ll 1$ and become uncorrelated when $k_m \simeq (\alpha\rho/\rho_n)^{3/2}/\eta$. As one sees in Table I, for all T in our simulation, $\alpha\rho/\rho_n \simeq 0.5$–$1.2$. Therefore, one should expect velocity locking for all T and for all $k_m \eta \lesssim 1$ including the enhancement range. This prediction agrees with our results.

This means that the origin for the variations of the scaling is not in the enhancement range but rather in the vicinity of the viscous cutoff, where $k_{m+} \sim k_\eta$. The key role is played by the energy dissipation due to the mutual friction $D_m^{\mathrm{MF}} = \alpha\rho_s\Omega_s|u_m^s - u_m^n|^2$, as follows from Eqs. (3a)–(3c). Clearly, $D_m^{\mathrm{MF}} \to 0$ for $T \to T_\lambda$ (because $\rho_s \to 0$) and for $T \to 0$ (because $\alpha \to 0$) and has a maximum at $T \simeq (0.80$–$0.85)T_\lambda$, i.e., in the range, where the intermittency enhancement is observed. Moreover, in this range, the total mutual friction dissipation $\sum_m D_m^{\mathrm{MF}}$ is close to (or even larger than) the total viscous dissipation $\nu_n \sum_m k_m^2 S_{2,m}^n$. Importantly, D_m^{MF} has a maximum at k_m, close to that of the viscous dissipation. As a result, for $T \simeq (0.80$–$0.85)T_\lambda$, the mutual friction between superfluid and normal components markedly drives the system away from the simple one-fluid behavior primarily around $k \sim k_\eta$, leading to a sharper decay of the energy spectrum $S_{2,m}^{n,s}$. In turn, this may give rise to a bottleneck effect leading to an energy accumulation near k_η. This phenomenon shares similarities with the bottleneck in classical fluids [21] but differs in important aspects: e.g., as in classical fluids the width of the energy accumulation range is almost independent of underlying mechanism and only its magnitude varies. In our case, however, the extent of the enhancement interval is much larger, about 3 decades, compared to 1 decade in classical fluids. A possible reason for such an extended enhancement interval is the energy transfer from superfluid to normal component, caused by mutual friction, and it is also notable in the same T range.

A more complete study of the quantitative aspects of the enhancement of intermittency requires an extensive analysis of the time dependencies of $u_m^s(t)$ and $u_m^n(t)$ in order to clarify the role of the mutual friction on the statistics of outliers, the main contributors to the fat tails of the PDFs which are responsible for the intermittency [22].

Summary.—Shell model simulations of the large-scale superfluid turbulence in ^{4}He indicate that for high- and low-T limits, when $\rho_s < 0.1\rho$ and $\rho_s > 0.9\rho$ the anomalous scaling exponents of superfluid turbulence coincide with their classical counterparts, as follows from our theoretical reasoning and in agreement with numerical and laboratory observations [10]. The shell model simulations allowed us to uncover considerable T-dependent variations of the apparent scaling over the enhancement interval of scales about 3 decades when $\rho_s \sim \rho_n$. This range can be characterized by the effective scaling exponents $\tilde{\xi}_p(T)$ that deviate further from the normal K41 values as compared to the exponents of classical fluids. Furthermore, if the entire inertial interval is shorter than the enhancement interval, only the effective scaling is observed. We also suggested Eq. (2) relating $\tilde{\xi}_p(T)$ to ξ_p.

While our interpretation indicates the existence of a form of the energy bottleneck in the two-fluid system, the phenomenon definitely calls for further investigation. Direct numerical simulations of superfluid turbulence oriented towards the study of the predicted T-dependent scaling over inertial interval of at least 2 decades is nowadays realistic and appears as particularly timely. Even more importantly, the temperature range $T \simeq (1.7$–$1.9)$ K, where we forecast a change in the scaling behavior, is accessible to laboratory experiments. We hope that the results presented in this Letter will inspire new numerical and laboratory studies of intermittency in superfluid turbulence.

This work is supported by the EU FP7 Microkelvin program (Project No. 228464)

[1] U. Frisch, *Turbulence, The Legacy of A. N. Kolomogorov* (Cambridge University Press, Cambridge, England, 1995).
[2] L. Landau, Phys. Rev. **60**, 356 (1941).
[3] W. F. Vinen and J. J. Niemela, J. Low Temp. Phys. **128**, 167 (2002).
[4] M. S. Paoletti and D. P. Lathrop, Annu. Rev. Condens. Matter Phys. **2**, 213 (2011).
[5] L. Skrbek and K. R. Sreenivasan, Phys. Fluids **24**, 011301 (2012).
[6] I. M. Khalatnikov, *Introduction to the Theory of Superfluidity* (Westerview Press, Boulder, Colorado, 2000).
[7] R. J. Donnelly, *Quantized Vortices in Helium II* (Cambridge University Press, Cambridge, England, 1991).
[8] W. F. Vinen, Proc. R. Soc. A **240**, 114 (1957); **240**, 128 (1957); **242**, 493 (1957).
[9] J. Maurer and P. Tabeling, Europhys. Lett. **43**, 29 (1998).
[10] J. Salort, B. Chabaud, E. Lévêque, and P.-E. Roche, J. Phys. Conf. Ser. **318**, 042014 (2011); Europhys. Lett. **97**, 34 006 (2012).
[11] B. Gledzer, Sov. Phys. Dokl. **18**, 216 (1973); M. Yamada and K. Ohkitani, J. Phys. Soc. Jpn. **56**, 4210 (1987).

[12] V. S. L'vov, E. Podivilov, A. Pomyalov, I. Procaccia, and D. Vandembroucq, Phys. Rev. E **58**, 1811 (1998).
[13] D. Pissarenko, L. Biferale, D. Courvoisier, U. Frisch, and M. Vergassola, Phys. Fluids A **5**, 2533 (1993).
[14] D. H. Wacks and C. F. Barenghi, Phys. Rev. B **84**, 184505 (2011).
[15] L. Boué, V. L'vov, A. Pomyalov, and I. Procaccia, Phys. Rev. B **85**, 104502 (2012).
[16] S. M. Cox and P. C. Matthews, J. Comput. Phys. **176**, 430 (2002).
[17] R. J. Donnelly and C. F. Barenghi, J. Phys. Chem. Ref. Data **27**, 6 (1998).
[18] Notice that we observe the energy accumulation for scales larger than intervortex distance ℓ, while in Ref. [19] it happens at smaller scales.
[19] A. W. Baggaley and C. F. Barenghi, Phys. Rev. E **84**, 067301 (2011).
[20] V. S. L'vov, S. V. Nazarenko, and L. Skrbek, J. Low Temp. Phys. **145**, 125 (2006).
[21] N. E. L. Haugen and A. Brandenburg, Phys. Rev. E **70**, 026405 (2004); U. Frisch, S. Kurien, R. Pandit, W. Pauls, S. S. Ray, A. Wirth, and J.-Z. Zhu, Phys. Rev. Lett. **101**, 144501 (2008).
[22] V. S. L'vov, A. Pomyalov, and I. Procaccia, Phys. Rev. E **63**, 056118 (2001).